Available online at www.sciencedirect.com
SCIENCE DIRECT®
Journal of Applied Geophysics 52 (2003) 1–9
JOURNAL OF APPLIED GEOPHYSICS
www.elsevier.com/locate/jappgeo

Semiquantitative evaluation of massive rock quality using ground penetrating radar

Luciana Orlando*

Dept. Idraulica Trasporti e Strade, University of Rome 'La Sapienza', Via Eudossiana 18, 00184 Rome, Italy

Received 26 March 2001; accepted 2 October 2002

Abstract

This work studies a methodology starting from georadar data that allows a semiquantitative evaluation of massive rock quality. The method is based on the concept that in good quality rock, most of the energy is transmitted, while in low quality rock, the energy is backscattered from fractures, strata joints, cavities, etc. When the energy loss due to spherical divergence and attenuation can be recovered by applying a constant spherical/exponential gain, the resulting energy function observed in the georadar section depends only on the backscattered energy. In such cases, it can be assumed that the amount of energy is an index of rock quality. Radar section interpretation is usually based on the reconstruction of reflected high-energy organized events. Thus, no consideration is given to backscattered not-organized energy produced by microfractures that greatly influences the geotechnical characteristics of the rock mass. In order to take into consideration all the backscattered energy, we propose a method based on the calculation of the average energy relative to a portion of predefined rock. The method allows a synthetic representation of the energy distributed throughout the section. The energy is computed as the sum of the square of amplitude of samplings contained inside cells of appropriate dimensions. The resultant section gives a synthetic and immediate mapping of rock quality. The consistency of the method has been tested by comparing georadar data acquired in travertine and limestone quarries, with seismic tomography and images of actual geological sections. The comparison highlights how effectively the energy calculated inside the cells give synthetic representation of the quality of rocks; this can result in maps where the high-energy values correspond to rock of poor quality and the low energy values correspond to a good quality region. The results obtained in this way can, in this case, be partly superimposed onto those of seismic tomography.

Keywords: Georadar; Quality of massive rocks; Backscattered energy

1. Introduction

The characterization of rock quality is most important in civil engineering (galleries, foundations, etc.) and in the assessment and restoration of archeological monuments, and the exploitation of ornamental rocks. In fact, knowledge of rock quality is useful to engineering work, both in the planning phase and, later, in the monitoring of rock characteristics. Furthermore, a good knowledge of the rock mass characteristics can be useful in ensuring a correct restoration of the damaged structure.

To establish structure stability, there is often recourse, in many cases in the projection and monitoring phases, to direct methods like drilling. However, such methods have the inconvenience of not always being applicable, of being very costly and of giving

* Fax: +39-6-44585080.
E-mail address: luciana.orlando@uniroma1.it (L. Orlando).

0926-9851/02/$ - see front matter © 2002 Elsevier Science B.V. All rights reserved.
PII: S0926-9851(02)00229-X

vertical information that cannot always be extrapolated to large areas. Therefore, more and more use is being made of indirect investigation methods that allow, with lower investment, the investigation of very large areas. Seismic refraction and tomography are the most popular of these indirect methods, and are based on estimating the degree of integrity of massive rock from elasticity parameters derived from velocity measurements (Bernabini and Borelli, 1974; Brizzolari, 1981; Nolet, 1987; Sattel et al., 1992; Cardarelli and de Nardis, 2001).

Seismic refraction techniques give velocity averages in rock over distances equal to the geofonic offset, while seismic tomography gives the velocity averages within the cell itself. The size of the cells is chosen on the basis of signal frequency and the number and length of travel in each cell; high resolution requires the generation and recording of high frequencies (Tarantola, 1987; Williamson, 1991; Williamson and Worthington, 1993). Seismic tomography often requires the drilling of holes. In any case, both methods estimate average velocities that are influenced mainly by diffused microfractures rather than by isolated single fractures. However, the detection of an isolated fracture and the reconstruction of its geometry can be very important, especially for the stability of buildings and for ornamental rock exploitation. In this case, an important role can be played by ground penetrating radar (GPR) based on the underground propagation of electromagnetic waves (Annan and Cosway, 1989). In georadar surveying, most of the energy of the electromagnetic wave is transmitted through integral rock, while in the case of fractured rock, i.e. rock of low quality, the energy is backscattered as a function of the dielectric characteristics of the material filling the cracks. This scattering may be organized or not, depending on the ratio between heterogeneity size and wavelength (Annan and Cosway, 1989; Olhoeft, 1998). The interpretation of georadar sections is normally made by evaluating the organized backscattered energy. In this way, events having greater lateral continuity and greater energy content are reconstructed. Generally speaking, such reconstruction ignores all lower energy and/or energy that is not organized. The results obtainable consist, essentially, in the representation of discontinuity like the contact between strata, cavities, main fractures, etc. (Bernabini et al., 1994; Botelho and Mufti, 1998; Deng et al., 1994; Davis and Annan, 1989; Casas et al., 1996; Grasmueck, 1996; Sigurdsson and Overgaard, 1996; Cappelli et al., 1998; Siggins, 1990a,b). The georadar interpretation does not generally highlight the backcattered energy and the diffraction from small cavities, diffused fractures, inclusions, etc., that influence the average characteristics of rock. From this aspect, the georadar method gives information complementary to that of seismic refraction and tomographic methods. A method to locate the fractured zone in massive rock using georadar was proposed by Grandjean and Gourry (1996) and Derobat and Abraham (2000). The method is based on the analysis of the amplitude envelope obtained from the Hilbert Transform.

In this work, we propose a method based on the analysis of the energy calculated as the square of the sample amplitude of the real trace. To produce a synthetic map of rock quality, the energy is calculated as the mean energy within portion of rock (cell). To test the consistency of the method, radar energy data are compared with the seismic tomographic data and the actual geological setting.

2. Theoretical analysis

As already mentioned, for integral rock, most of the electromagnetic wave energy is transmitted, whereas in damaged rock, i.e. rock of poor quality, the energy becomes backscattered as a function of the dielectric characteristics of the filler material (air, water, clay). The scattering can be organized or not, depending on the ratio between the heterogeneity size and wavelength (Olhoeft, 1998; Annan and Cosway, 1989). In this way, the inverse correspondence between the level of scattering in the radar sections and the quality of the rock can be identified.

The radar sections contain multitudes of reflections, but only those with high, organized energy are usually taken into account in the interpretation of data. Thus, only a part of all the information contained in the radar section is considered. The user is often interested in having an indication not only of the main discontinuities but also a synthetic evaluation of the quality of all the rock mass. As the energy of the backscattering reflections is tied directly to the quality of the rock, the higher the energy the lower the quality, and vice versa.

Therefore, the estimation of the energy at each point in the section could be a useful tool in evaluating rock quality. To have a synthetic map for rock quality comparable with the results obtainable from seismic tomographic methods, and in which all the backscattered energy is taken into account, our proposal is to synthesize an energy map, averaging the energy within appropriately portioned rock (cell in the section). This average energy can be considered as an average evaluation of the discontinuities present within the cells. The thus calculated energy map can therefore give an immediate synthetic semiquantitative evaluation of the rock quality. In this, easily read representation where all the discontinuities contained in the rock have been considered. The level of synthesis is a function of cell size, however, the minimum size dimension must be chosen as a function of the horizontal and lateral resolution of the radar data.

On drawing a parallel between the radar energy calculated within cells and that from the tomographic seismic section, we find that the radar section of integral rock shows a low energy level and the tomography reveals high velocity. In poor quality rock, i.e. highly fractured, the radar sections show a high level of energy and the tomography gives low velocity. The energy section could be comparable with that obtained from seismic tomographic method.

Obviously, the energy maps are of objective validity only in the case of resistive rock where the attenuation of the energy with depth can be recovered by a gain function constant for each profile. To verify whether the radar energy sections are really comparable with the seismic tomography and correspond to the actual geological setting, the radar energy maps have been compared with both tomographic seismic surveys and geological sections.

3. Acquisition and processing of data

The data shown in the present paper were acquired in travertine and limestone quarries and in tunnels excavated in limestone.

The travertine quarry, high porosity lacustrine stratified calcium carbonate strata 2–8 m thick, interbedded with varying thicknesses of clay, is characterized by sets of fractures, isolated fractures and karst cavities.

The limestone quarry consists of 2–6-m-thick strata interbedded with thin clay layers; these limestone strata are affected by two different sets (WSW and NNE) of nearly vertical fractures (between 50° and 90°).

In travertine and limestone open quarries, the data were acquired in continuous mode at the top of the bench at a distance of 2–4 m from the vertical cut of bench. The horizontal sampling is about 20 traces per meter.

The tunnel, constructed in the 1930s, was excavated in limestone to catch drinking water; two near vertical sets of fractures are present in the limestone. The studied area is a slice of rock about 80×12 m in size, delimited by tunnels as can be seen in the map of Fig. 2. In several zones, the fractures caused a cataclysm of the limestone that led to stability problems in the tunnels. During the Central Apennines earthquake (1997), a cave-in occurred in the tunnel ‘Longitudinale alta’ and the debris blocked part of the tunnel making it unusable (gray zone in Fig. 2).

The reflection radar section in the tunnel was acquired in step mode along the wall of the tunnel ‘‘Longitudinale bassa’’ (see Fig. 2 for location). The horizontal sampling was one trace every 0.10 m.

In all sites, the data were acquired with 200-MHz antenna in true amplitude and without applying any lateral and vertical filters.

The velocities are of 0.08–0.09 m/ns in the travertine quarry and 0.09–0.1 m/ns in the limestone quarry and tunnel. The velocity in travertine was carried out from CMP analysis (Fig. 1) in limestone quarry from diffraction hyperbola and in limestone tunnel from the ratio of known distance between the opposite walls of tunnels ‘Longitudinale bassa’ and ‘Longitudinale alta’ and the time reflection from the wall of tunnel ‘Longitudinale bassa’ (Fig. 2). The spectra analyses give peak frequencies between 110 and 150 MHz in each site.

As stated earlier, the method is based on the analysis of the energy level in the section; this means that for such analyses to be significant, it is necessary to recover the energy loss that occurs with depth for spherical divergence and attenuation. As in the specific case, the resistivity in the limestone and travertine rocks is greater than 300 Ω m, and the band frequency of signal is between 80 and 200 MHz. We hypothesized that the attenuation is independent of the

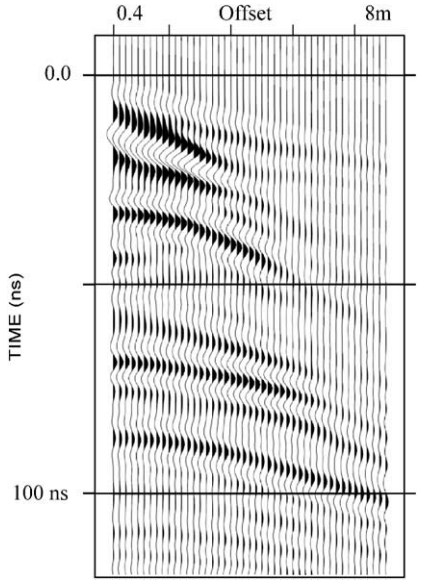

Fig. 1. Common Mid Point (CMP) acquired in travertine quarry.

frequency and that the energy loss due to attenuation can be recovered by exponential gain and the spherical divergence by spherical gain.

The processing applied to the radar data was:

(1) dewow and low pass filter,
(2) spherical/exponential gain,
(3) FK migration,
(4) energy computation.

The optimum gain, constant for each profile, was chosen as an inverse function of the loss in energy with depth, evaluated as the mean of all traces.

The migration was achieved by applying the FK algorithm (Stolt, 1978) assuming a constant velocity for each record of 0.09 m/ns.

To calculate the energy, the radar data were divided into cells defined by a temporal interval (determined by a number of constant samplings) and by a spatial interval (determined by a number of constant traces). For each cell, the average energy was calculated as the sum of the squares of amplitude contained in each cell. Therefore, the energy was computed using the following equation:

$$\text{Energy}\ (k) = 1/N\left(\sum\sum(A_{i,j})^2\right)$$

where k is the k-esima cell, $A_{i,j}$ is the amplitude of the sampling i of trace j, N is the number of samples inside the cell. The summation is extended to all the samples included in the temporal and spatial interval belonging to the traces of the considered k-esima cell.

The size of the cells was chosen as a function of the lateral and vertical resolution of the data. Considering the velocity of the electromagnetic wave and the central frequency of the antenna, it was considered that the minimum resolution obtainable can be achieved by using cells about 0.5 m wide. On the computation of energy, the first 20 ns was not taken into account because of their high energy due to not-shielded antenna.

4. Data analysis

The early analysis is to compare the tomographic seismic data with the radar energy acquired in the tunnel excavated in limestone. The seismic tomographic survey was acquired along the walls of the tunnels delimiting the rock mass in such a way as to involve the same plane investigated by the georadar. For the acquisition parameters and inversion algorithms used for the seismic tomography, the reader is referred to the work of Cardarelli et al. (submitted for publication). The resolution obtained by the tomographic survey is given by the cell size, the sides varying between 1 and 3 m.

Fig. 2 shows the GPR migrated record, map energy and seismic tomography. At the top is the georadar migrated section acquired along the wall of the tunnel (A–B in Fig. 2). The georadar data were acquired along a horizontal profile located on the wall of the 'Longitudinale bassa' tunnel. The 52-m-long profile was acquired by trace sampling every 0.10 m. The event 1 is the reflection from the wall of the tunnel 'Longitudinale alta'. The radar survey detected many reflections and diffractions due to fractures and cavities present in the limestone.

At the center of the figure (Fig. 2b), the energy map, calculated considering 0.5-m-sized cells, is shown. In this map, to eliminate the high energy due to direct airwave, the first 20 ns (1 m) of the radar section was cut. It can be seen that the energy section (Fig. 2b) synthesizes the information already present in the migrated radar section (Fig. 2a). The red

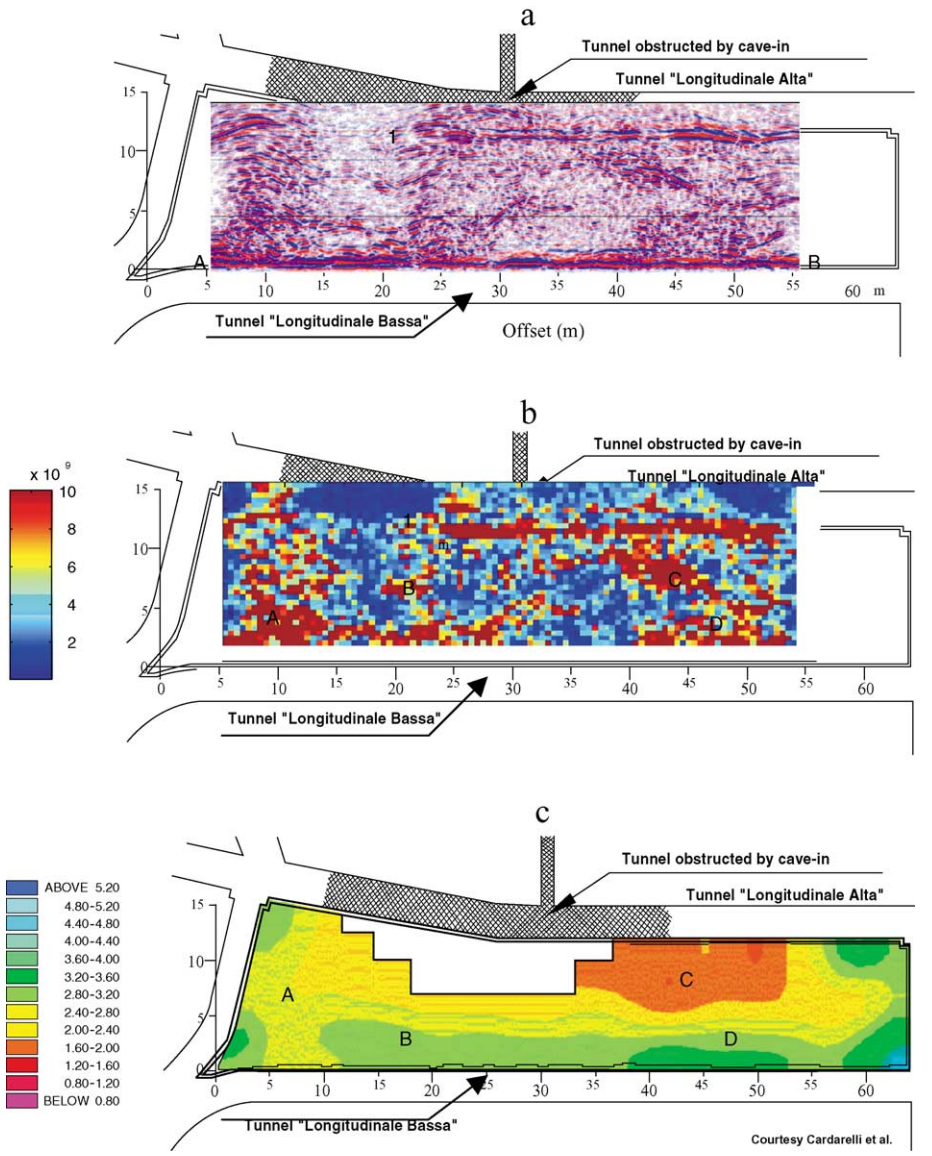

Fig. 2. At the top (a), 200 MHz migrated radar section acquired along the wall of tunnel excavated in limestone is shown. A–B indicates the location of the radar profile. The data are acquired in step mode with a trace every 0.10 m. In (b), the energy map is calculated as the sum of the squared of amplitude contained in cell of 0.5 m wide. In the energy map, the first 30 ns was cut. At the bottom (c), the seismic tomography is shown. The map of tunnels is drawn. The gray zone indicates the obstructed tunnel zone of tunnel 'Longitudinale alta'.

pixels correspond to cells of high energy, while the blue cells correspond to cells with low energy. The velocity from the seismic tomography is shown at the bottom of Fig. 2c; low velocity zones are in red, high are in green. The former correlates with rock of low quality, the latter with good quality. Because the 'Longitudinale alta' tunnel was partly obstructed by cave-in detritus, the white area in Fig. 2c was not investigated by tomographic survey.

On comparing the energy (Fig. 2b) and tomography maps (Fig. 2c), we observe a good overlapping of the results, these being the same in A, D and C using

both methods. In B, there is no correspondence. In this zone, the energy map indicates rock of low quality while the tomography indicates good quality. The not-perfect correspondence in B is probably due to the small number of seismic rays in this area.

It should be pointed out that a complete superimposition of the results is not possible, in that the resolution of the two methods differs, mainly in the zone close to the wall of the tunnel where, in the radar section, the direct wave occurs.

Fig. 3 enables a comparison of the energy maps and the actual data obtained from photographic images of the vertical cut of limestone bench. The top of Fig. 3 shows a photographic image of the vertical cut of a limestone quarry bench where there is a set of fractures filled with clayey material. The radar section, acquired parallel to the quarry wall and 4 m away from it, can be seen in Fig. 3b. A high numbers of diffraction hyperbola are present in correspondence with the set of fractures of Fig. 3a. In the migrated

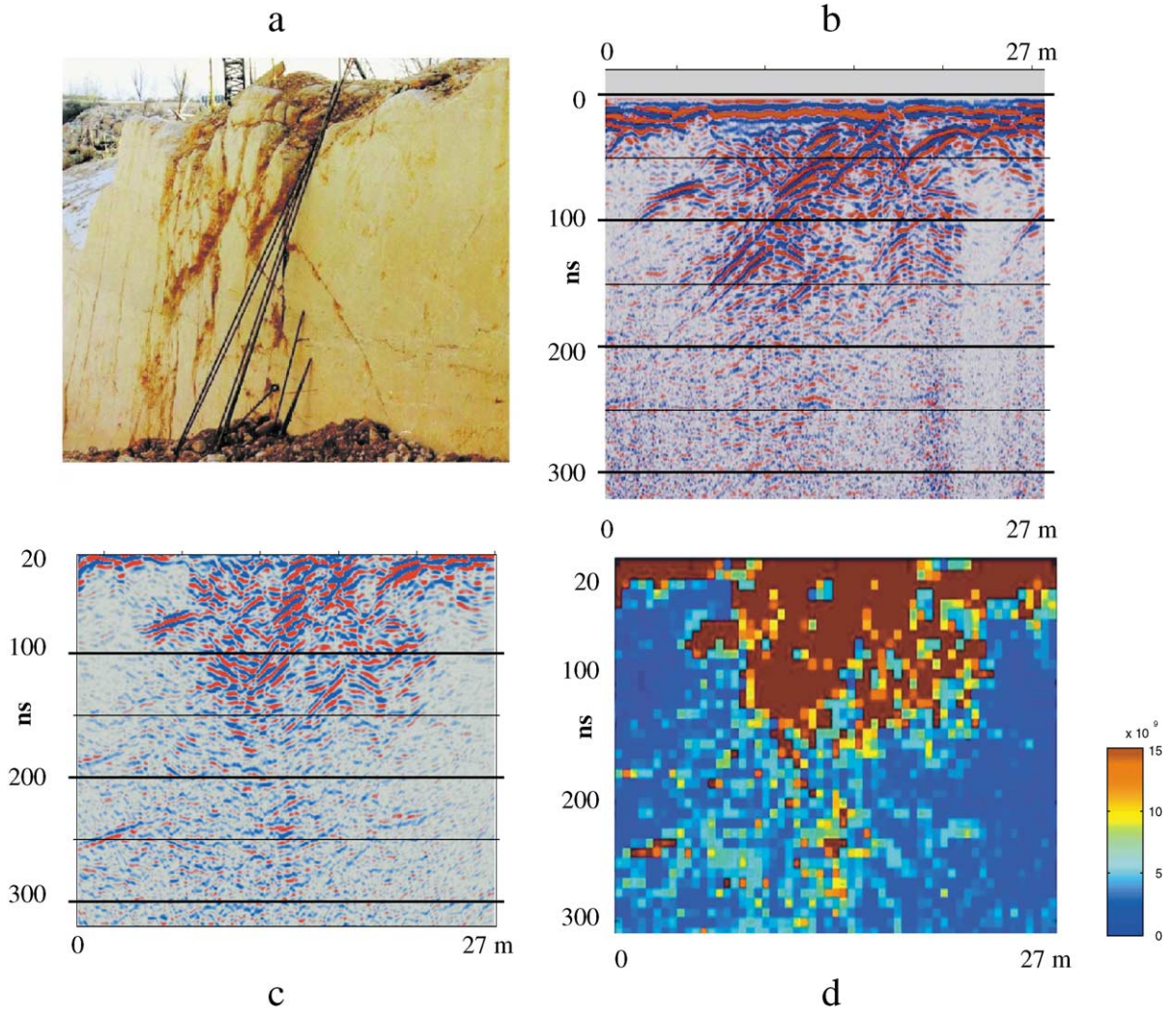

Fig. 3. At the top (a), the photo image of the limestone rock face is shown. In the image, a set of fractures filled with clay can be recognized; (b) shows the radar section acquired on top of the bench at a distance of 4 m and parallel to the vertical face quarry. Fractures produce a lot of diffraction hyperbolas. In (c), the migrated section is shown. In (d), the energy map obtained from the radar section of (c) is shown. In the energy map, the first 20 ns was cut.

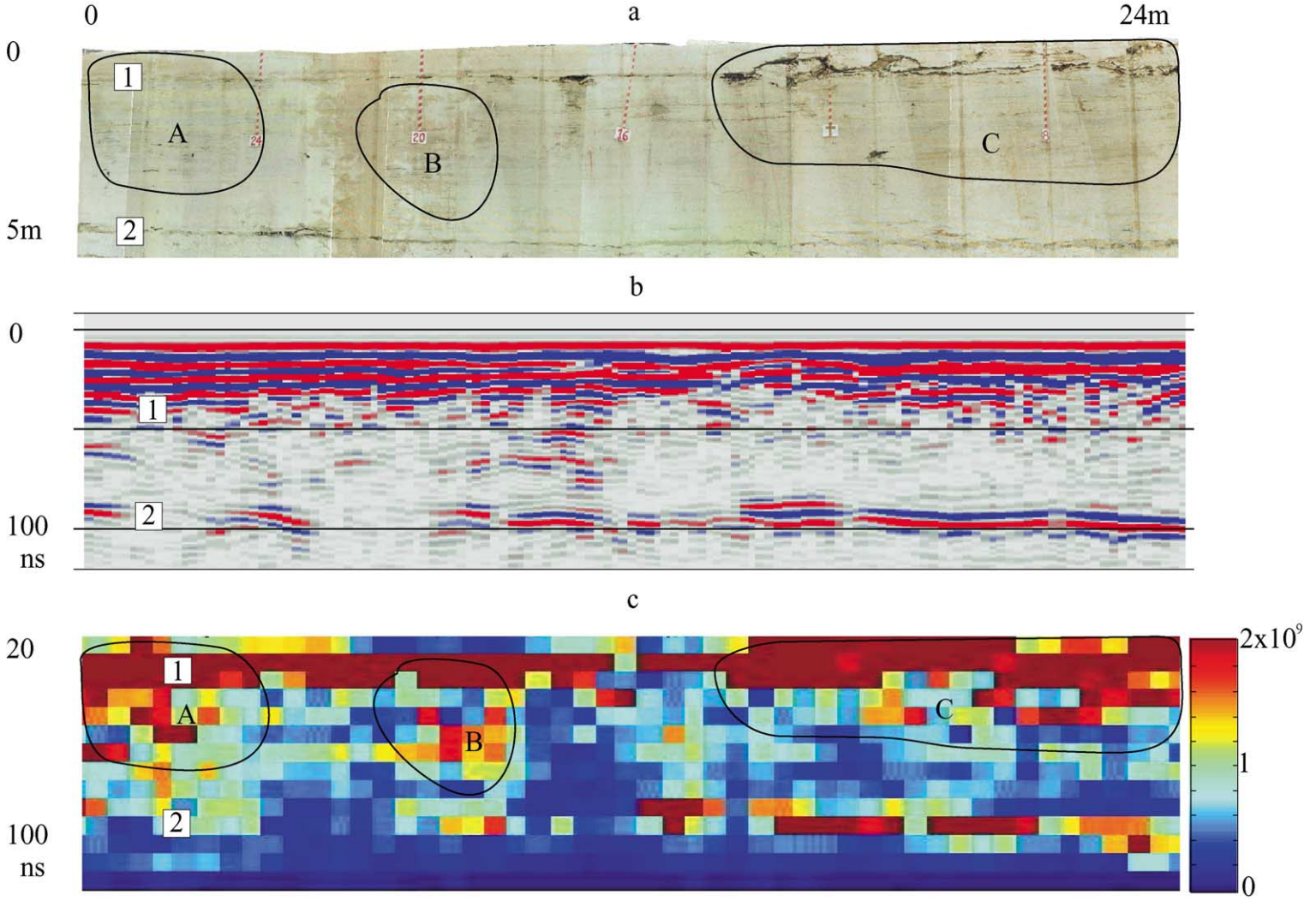

Fig. 4. At the top (a), the photo image of the travertine rock face is shown. In the image, a stratified-fractured deposit can be recognized; (b) shows the radar section acquired on top of the bench at a distance of 4 m and parallel to the vertical face quarry. At the bottom (c), the energy map obtained from the radar section of (b) is shown. In the energy map, the first 20 ns was cut. Energy map detects micro-fractured zones A and B.

section (Fig. 3c), the energy is focused. In Fig. 3d, the radar energy section of Fig. 3c is shown. An excellent correspondence between the energy map and the geological section is observable.

Fig. 4a shows the geological image of the travertine quarry; in this section, a lot of joint strata are present, the main ones are indicated in the figure with numbers (1–2). Subhorizontal microfractures are present in zones A and B. The joints are detected by the radar section (Fig. 4b) acquired on the top of the bench at a distance of 4 m from the vertical cut depicted in Fig. 4a. The radar section is not able to define the boundaries of micro-fractured zones A and B. As in this case, diffraction hyperbola and deep strata are not present; the energy map is carried out from the non-migrated section. The energy map detects the micro-fractured zones A and B. Also, in this case, the energy map synthesizes the rock quality correctly.

5. Conclusion

From the above examples, it can be seen that a good, immediate synthetic and inexpensive tool for evaluating massive rock quality lies in analyzing the map of average energy calculated within the cells obtained from the radar reflection section. This method is valid when noise is not very high, and the energy dissipated through attenuation and spherical divergence with depth can be recovered by an exponential/spherical gain. As scattering and attenuation are a function of the wavelength of the emitted signal, the choice of antenna to use for such types of prospecting becomes quite crucial. For complex geometry, it is enough to calculate the energy map from the migrated section. In the specific case, it was seen that the energy map acquired with the 200-MHz antenna gave a response comparable to that of seismic tomography. The next step could be to compute energy maps from radar data acquired using different frequency antenna so as to evaluate the degree of obtainable resolution.

References

Annan, A.P., Cosway, S.W., 1989. Ground penetrating radar for high resolution mapping of soil and rock stratigraphy. Geophysical Prospecting 37, 531–541.

Bernabini, M., Borelli, G.B., 1974. Methods for determining the average dynamic elastic properties of fractured rock mass and the variations of these properties near excavations. Proceeding of International Society for Rock Mechanics, Denver II, 393–397.

Bernabini, M., Brizzolari, E., Orlando, L., Santellani, G., 1994. Application of ground penetrating radar on Colosseum pillars. Proceeding of the Fifth International Conference on Ground Penetrating Radar, vol. 2, pp. 547–558.

Botelho, M.A.B., Mufti, I.R., 1998. Exploitation of limestone quarries in Brazil with depth migrated ground-penetrating radar data. 68th Annual International Meeting, Society of Exploration Geophysicists, Expanded Abstracts, pp. 836–839.

Brizzolari, E., 1981. Miniseimic investigations in tunnels: methodology and results. Geoexploration 18, 259–267.

Cappelli, A., Di Fiore, L., Orlando, L., Saviano, G., Violo, M., 1998. Caretterizzazione merceologica e indagine dello stato di fratturazione mediante georadar. Quarry and Construction, October, 7–17.

Cardarelli, E., de Nardis, R., 2001. Seismic refraction, and isotropic and anisotropic seismic tomography on ancient monument (Antonino and Faustina temple AD 141). Geophysical Prospecting 49, 1–14.

Cardarelli, E., Marrone, C., Orlando, L., 2001. Evaluation of tunnel stability using integrated geophysical methods. Journal of Applied Geophysics (submitted for publication).

Casas, A., Lazaro, R., Vilas, M., Busquet, E., 1996. Detecting karstic cavities with ground penetrating radar at different environments in Spain. Proceeding of 6th International Conference on Ground Penetrating Radar Japan, pp. 455–460.

Davis, J.L., Annan, A.P., 1989. Ground-penetrating radar for high-resolution mapping of soil and rock stratigraphy. Geophysical Prospecting 37 (05), 531–552.

Deng, S., Zuo, Z., Wang, H., 1994. The application of ground penetrating radar to the detection of shallow faults and cavities. Proceeding of 5th International Conference on Ground Penetrating Radar, Ontario Canada, vol. 3, pp. 1115–1120.

Derobat, X., Abraham, O., 2000. GPR and seismic imaging in a gypsum quarry. Journal of Applied Geophysics 45, 157–169.

Grandjean, G., Gourry, J.C., 1996. GPR data processing for 3D fracture mapping in a marble quarry (Thassos, Greece). Journal of Applied Geophysics 36, 19–30.

Grasmueck, M., 1996. 3-D ground-penetrating radar applied to fracture imaging in gneiss. Geophysics 61 (04), 1050–1064.

Nolet, G., 1987. Seismic wave propagation and seismic tomography. In: Nolet, G. (Ed.), Seismic Tomography. Reidel, pp. 1–23.

Olhoeft, G.P., 1998. Electrical, magnetic, and geometric properties that determine ground penetrating radar performance. Proceeding of 7th International Conference on Ground Penetrating Radar, Lawrence, USA, pp. 27–30.

Sattel, G., Frey, P., Amberg, R., 1992. Prediction ahead of the tunnel face by seismic methods—pilot project in Centovalli Tunnel, Switzerland. First Break 10 (01), 19–25.

Siggins, A.F., 1990a. A radar investigation of fracture in a granite outcrop. Exploration Geophysics 21 (1/2), 105–110.

Siggins, A.F., 1990b. Ground-penetrating radar in geotechnical applications. Exploration Geophysics 21 (3/4), 175–186.

Sigurdsson, T., Overgaard, T., 1996. Application of GPR for 3D visualization of geological structural variation in a limestone formation. Proceeding of 6th International Conference on Ground Penetrating Radar Sendai, Japan, pp. 39–44.

Stolt, R.H., 1978. Migration by Fourier transform. Geophysics 43, 23–48.

Tarantola, A., 1987. Inverse Problem Theory. Elsevier.

Williamson, P.R., 1991. A guide to the limits of resolution imposed by scattering in ray tomography. Geophysics 56, 202–207.

Williamson, P.R., Worthington, M.H., 1993. Resolution limits in ray tomography due to wave behavior. Numerical experiments. Geophysics 58, 727–735.